



HAL
open science

A Novel Approach To Quantify Air–Water Gas Exchange in Shallow Surface Waters Using High-Resolution Time Series of Dissolved Atmospheric Gases

Ulrich Weber, Peter Cook, Matthias Brennwald, Rolf Kipfer, Thomas Stieglitz

► **To cite this version:**

Ulrich Weber, Peter Cook, Matthias Brennwald, Rolf Kipfer, Thomas Stieglitz. A Novel Approach To Quantify Air–Water Gas Exchange in Shallow Surface Waters Using High-Resolution Time Series of Dissolved Atmospheric Gases. *Environmental Science and Technology*, 2019, 53 (3), pp.1463-1470. 10.1021/acs.est.8b05318 . hal-01986368

HAL Id: hal-01986368

<https://hal.science/hal-01986368v1>

Submitted on 25 Jan 2019

HAL is a multi-disciplinary open access archive for the deposit and dissemination of scientific research documents, whether they are published or not. The documents may come from teaching and research institutions in France or abroad, or from public or private research centers.

L'archive ouverte pluridisciplinaire **HAL**, est destinée au dépôt et à la diffusion de documents scientifiques de niveau recherche, publiés ou non, émanant des établissements d'enseignement et de recherche français ou étrangers, des laboratoires publics ou privés.

A Novel Approach to Quantify Air-Water Gas Exchange in Shallow Surface Waters Using High-Resolution Time Series of Dissolved Atmospheric Gases

Ulrich W. Weber,^{*,‡} Peter G. Cook,^{¶,§} Matthias S. Brennwald,[‡] Rolf Kipfer,^{‡,||} and Thomas C. Stieglitz^{⊥, #}

[‡]*Department of Water Resources and Drinking Water, Eawag, Swiss Federal Institute of Aquatic Science and Technology, Dübendorf 8600, Switzerland*

[¶]*National Centre for Groundwater Research and Training (NCGRT), School of the Environment, Flinders University, Adelaide SA 5001, Australia*

[§]*Aix-Marseille Université, IMéRA, Marseille 13004, France*

^{||}*Institute for Geochemistry and Petrology, ETH Zurich, Zurich 8092, Switzerland*

[⊥]*Centre Européen de Recherche et d'Enseignement des Géosciences de l'Environnement (CEREGE), CNRS, IRD, INRA, Coll France, Aix en Provence 13545, France*

[#]*Centre for Tropical Water and Aquatic Ecosystem Research, James Cook University, Townsville QLD 4811, Australia*

E-mail: uli.weber@eawag.ch

Phone: +49 (0) 176 99123345

Abstract

Gas exchange across the air-water interface is a key process determining the release of greenhouse gases from surface waters, and a fundamental component of gas dynamics

5 in aquatic systems. In order to experimentally quantify the gas transfer velocity in a
6 wide range of aquatic settings, a novel method is presented based on recently developed
7 techniques for the *in situ*, near-continuous measurement of dissolved (noble) gases with
8 a field-portable mass spectrometer.

9 Variations in observed dissolved gas concentrations are damped and lagged with
10 respect to equilibrium concentrations, being the result of (a) temperature (and thus
11 solubility) variations, (b) water depth and (c) the specific gas transfer velocity (k_i).
12 The method fits a model to the measured gas concentrations to derive the gas transfer
13 velocity from the amplitude and the phase lag between observed and equilibrium con-
14 centrations. With the current experimental setup, the method is ~~most~~ sensitive to gas
15 transfer velocities of ~~0.1—8 m/h~~0.05—9 m/d (for N_2), at a water depth of 1 m, and a
16 given daily water temperature variation of 10 °C. Experiments were carried out (a) in a
17 controlled experiment to prove the concept and to confirm the capability to determine
18 low transfer velocities and (b) in a field study in a shallow coastal lagoon covering a
19 range of transfer velocities, demonstrating the field applicability of the method.

20 Introduction

21 Gas exchange across the air-water interface is a key process coupling atmospheric and aquatic
22 gas cycles. Accurate knowledge of gas exchange rates, ~~expressed by the gas transfer velocity~~
23 is required to determine mass balances of dissolved gases in aquatic systems, which can in
24 turn be used to estimate fluxes between groundwater reservoirs and surface water^{1,2}1-3. Sur-
25 face water bodies can be sources or sinks for gases:^{4,5} whereas release of methane and carbon
26 dioxide from water bodies is an important source of greenhouse gases to the atmosphere,
27 the reverse flux of oxygen and nitrogen from atmosphere to water is an important factor in
28 water quality and ecosystem functioning.⁶

29 The gas transfer velocity for open ocean conditions is well parametrized in its dependence
30 on wind speed.⁷ Furthermore, numerous empirical relationships are available for rivers where

31 gas exchange is primarily a function of turbulent mixing due to water flow.⁸ In contrast, for
32 shallow open water surfaces like shallow lakes and, importantly, the coastal zone of oceans, a
33 parametrization is currently not available that fully takes into account the physical processes
34 driving gas exchange, which differ significantly from those in the open ocean or rivers. In
35 these systems, the influence of other environmental parameters, e.g. rain,^{9,10} current veloc-
36 ity or bottom roughness, on near surface turbulence increases due to the decreased wind
37 fetch and lower water depth,¹¹ ~~which fundamentally impact and this fundamentally impacts~~
38 air/water partitioning.

39 A commonly used method for estimating the transfer velocity at specific sites over short
40 time scales consists of injecting ~~trace gases (e.g. the ³He/SF₆ dual tracer technique^{11,12}) and~~
41 ~~monitoring their rate of removal by air-water gas exchange¹³. These methods are subject~~
42 ~~to a number of experimental challenges and limitations, and monitoring trace gases¹¹⁻¹⁴.~~
43 Besides being experimentally demanding¹¹ and sometimes being subject to environmental
44 regulation (e.g. the identification of the exact geometry of the tracer patch¹¹. Additionally,
45 ~~injection of gas tracers in surface water contaminates the site and future use of those gases~~
46 ~~as natural groundwater tracers may become SF₆), trace gas injection may contaminate the~~
47 sites and render future experiments impossible.¹⁵ Further, the use of artificial tracers (e.g.
48 ~~SF₆) is becoming increasingly regulated.~~

49 Recently, in studies primarily targeting the estimation of residence times of water within
50 catchments, it was noted that diurnal variations in water temperature in rivers produced
51 periodically varying concentrations of dissolved gases, which were damped and lagged ~~to the~~
52 ~~respective atmospheric equilibrium concentration~~ in comparison with atmospheric equilibrium
53 concentrations.¹⁵

54 Variations of the gas concentrations are a function of the temperature variation, the
55 temperature-dependence of gas solubility in water, and the gas transfer velocity. In principle,
56 synchronous measurement of time series of temperature and concentrations of dissolved gases
57 therefore allows the gas transfer velocity to be estimated. ~~In the aforementioned study¹⁵,~~

58 ~~water samples were collected hourly over a 12-hour period, and the samples were analyzed~~
59 ~~in the laboratory for CFC, N₂ and Ar concentrations.~~ Recent advances in determining gas
60 concentrations have led to the development of field portable MIMS (membrane inlet mass
61 spectrometry) systems that can measure concentrations of He, Ar, Kr, N₂, O₂, CO₂ and
62 CH₄ with relatively high accuracy and precision.¹⁶⁻¹⁸ These novel techniques allow in-situ,
63 real-time measurement of gas concentration time series with a temporal resolution of a few
64 minutes and make subsequent laboratory analysis redundant.

65 The objective of this study is to combine the approach to calculate gas exchange rates
66 ¹⁵ with those novel measurement techniques. Further, we aim to establish the environmental
67 conditions for which gas transfer velocities can be derived using the diurnal gas dynamics
68 (DGD). ~~Our data make a strong case that measurements of changes in gas concentrations~~
69 ~~over time can indeed be used to determine the gas transfer velocity, and to identify temporal~~
70 ~~variations in gas transfer velocity in response to changing environmental conditions.~~ The
71 ~~introduced DGD method is applicable in rivers, in shallow lakes and lagoons, where well-mixed~~
72 ~~water conditions prevail, and avoids the injection of artificial tracers.~~

73 We first calculate the sensitivity and resolution of the presented method in a theoretical
74 setting. The performance and the experimental requirements ~~of the suggested method are~~
75 are then demonstrated in a controlled experiment and in the large, shallow La Palme lagoon
76 at the Mediterranean Sea in southern France.

77 Theory

78 The gas flux of species i between air and water is caused by a disequilibrium of aquatic and
79 atmospheric gas concentrations:¹⁹

$$F_i = k_i \cdot \Delta C_i = k_i \cdot (C_{w,i} - C_{eq,i}), \quad (1)$$

80 with F_i being the gas flux, $C_{w,i}$ the concentration in the water, and $C_{eq,i}$ the concentration
 81 in air saturated water, and k_i is the gas transfer velocity, which reflects the rate of exchange.
 82 This basic relation, even though not accounting for bubble-mediated gas fluxes, is used to
 83 determine fluxes at regional-to-global scales.⁷

84 If the water is well mixed, the flux can also be written as

$$F_i = \frac{dC_{w,i}}{dt} \cdot h, \quad (2)$$

85 with h being the water depth of the exchanging water mass ('mixed layer'). Equating 1 and
 86 2 yields

$$\frac{dC_{w,i}}{dt} = \frac{k_i}{h} \cdot (C_{w,i} - C_{eq,i}). \quad (3)$$

87 The equilibrium gas concentrations depend on the temperature (T_w) and the salinity (S)
 88 of the water and the partial pressure of ~~the gas~~, and is each gas, and are determined by
 89 Henry's law,²⁰

$$C_{eq,i} = \frac{p_i}{H_i(T_w, S)}. \quad (4)$$

90 The Henry's coefficient (H_i) is specific to each gas species.²¹⁻²³ p_i is the partial pressure of
 91 species i in the atmosphere and is given by $p_i = (p_{atm} - e_s(T_w))v_i$, with p_{atm} the local total
 92 atmospheric pressure, $e_s(T_w)$ the water vapor pressure, and v_i the volume fraction of gas i
 93 in dry air.²⁰

94 Diurnal variation in $C_{eq,i}$ for the different gases is largely a function of the temperature
 95 dependence of their solubilities²⁰. The magnitude of the diurnal variation in $C_{eq,i}$ for the
 96 noble gases will therefore be greatest for Xe and Kr, less for Ar and least for He and Ne.
 97 The temperature dependence of the solubility of N_2 is similar to that of Ar.

98 To convert the transfer velocity derived from one gas species to another commonly the
 99 respective Schmidt numbers are used. The Schmidt number is defined as the ratio of kine-
 100 matic viscosity of water, divided by the diffusion coefficient of the gas in water. The transfer
 101 velocities ($k_{1,2}$) of gas 1 and 2 are linked to each other via their Schmidt numbers ($Sc_{1,2}$) in

102 a power law dependence with the Schmidt number exponent (n):

$$\frac{k_1}{k_2} = \left(\frac{Sc_1}{Sc_2} \right)^{-n} \quad (5)$$

103 where n theoretically ranges from $1/2 < n < 2/3$, ~~theoretically~~²⁴. However, ~~it~~ n decreases
104 rapidly to $1/2$ ~~for~~ with the onset of waves²⁴ (free surface condition). The ratio of (Sc_1/Sc_2)
105 is approximately constant with temperature.²⁵

106 While concentration gradients for reactive gases can also occur due to biogeochemical
107 reactions, i.e. photosynthetic production in the case of O_2 and production by denitrification
108 in the case of N_2 , the concentrations of the (atmospheric) noble gases are only controlled by
109 physical processes, specifically radioactive decay and air-water gas-exchange.

110 Method

111 Modeling

112 An ordinary differential equation solver is used to derive the results for the expected in-situ
113 concentrations ($C_{w,i}$) by solving Eq. 3. The mean of the first ten measured $C_{w,i}$ of a time
114 series is used as the initial gas concentration.

115 The parameters for the equilibrium concentrations ($C_{eq,i}$) (cf. Eq. 4) and the water
116 depth are given by the local environmental system, so that the transfer velocity (k_i) and
117 $C_{w,i}$ remain as the only free parameters.

118 The model is fit to the measured concentrations by varying k_i . The fit is optimized by
119 minimizing the sum of squared errors (SSE) between the measured and modeled concentra-
120 tions of the respective gas species.

121 The uncertainty of the best-fit gas exchange rate k_i^* (95% confidence interval) was deter-
122 mined from the scatter of the observed concentrations relative to the best-fit model curves.²⁶

123 The measured gas concentrations time series of the field study were filtered with a Savitzky-

124 Golay filter (order 3, frame length 21) to reduce noise.²⁷

125 **Experimental Method**

126 The concentrations of dissolved N_2 , ^{40}Ar and ^{84}Kr in the water were analyzed with a
127 portable ‘miniRUEDI’ mass spectrometer¹⁶ (Gasometrix GmbH) using the gas-equilibrium
128 membrane-inlet mass spectrometry method (GE-MIMS).^{16,28,29} For later calculations ^{40}Ar
129 and ^{84}Kr are converted to elemental concentration.²⁰

130 During the experiments a submersible pump was used to continuously sample the water
131 through a membrane contactor module (Liqui-Cel G542), in which the gases equilibrate
132 between the water and a small gas headspace according to Henry’s law. The partial pressures
133 of N_2 , ^{40}Ar and ^{84}Kr in the headspace were quantified from the mass spectrometer readings
134 by peak-height comparison relative to analyses of ambient air, which was used as calibration
135 standard.¹⁶ The analytical sequence was ~~set to~~ a continuously repeating cycle consisting of
136 one air-standard analysis block, followed by three water sample analysis blocks, followed by
137 one ambient air sample analysis block to assess the analytical performance¹⁶. Each of these
138 analysis blocks were 8 *min* long.

139 The partial pressures observed in the headspaces of the membrane modules were con-
140 verted to dissolved gas concentrations using the gas-specific Henry’s law coefficients at the
141 temperature of the water in the membrane modules. The partial pressures obtained from the
142 ambient-air samples were used to estimate the analytical uncertainties of the dissolved-gas
143 concentrations as 1 % for N_2 , 2.5 % for Ar and 4 % for Kr.

144 In the controlled experiment and the field study at La Palme lagoon, in-situ water tem-
145 perature, salinity and atmospheric pressure were recorded by sensors every 10 *min* in order
146 to calculate $C_{eq,i}$ using Eq. 4.

147 **Controlled Experiment**

148 A concept test of the DGD method to determine gas transfer velocities was conducted
149 outside the Swiss Federal Institute of Aquatic Science and Technology (Eawag) in Dübendorf,
150 Switzerland. For that purpose, a small tank (*height = 15 cm, length = 60 cm, width =*
151 *40 cm*) with a black shell was used. The small volume (0.036 m^3) and the black color of the
152 tank caused a large temperature increase of the water in response to sun irradiation and a
153 rapid decline in water temperature as air temperature dropped at night.

154 The water in the tub was circulated through the membrane module, where the gases
155 equilibrate for measurement. The forced circulation caused an increase in turbulence in the
156 water, producing a well mixed water body. This turbulence is assumed to be constant over
157 time, as the pumping rate was kept constant. The development of (breaking) waves was
158 heavily suppressed by the walls and the small surface area of the tank.

159 **Field Study at La Palme Lagoon**

160 The DGD method was further applied during a field campaign in June 2017 at La Palme
161 lagoon on the French coastline of the Mediterranean Sea. The shallow lagoon has a surface
162 area of approximately 5 km^2 , a mean depth of 0.6 m and a maximum depth of 1.8 m .¹ The
163 water level was not influenced by tides, as there was no direct hydraulic connection of the
164 lagoon to the sea.

165 The small depth of the lagoon ensures the water heats up quickly in response to solar
166 irradiation and loses heat quickly at night, which leads to large diurnal temperature varia-
167 tions. The lagoon is regularly exposed to strong north-westerly winds, which cause waves of
168 a maximum amplitude of about 0.4 m .¹ Inflow of groundwater occurs in the northern section
169 of the lagoon.¹ Recirculation of water between the lagoon and the pore space of shallow sed-
170 iments is considerable ^{1,30}. ~~This and flows vary with up to an order of magnitude^{1,30}. Such~~
171 ~~water exchange might influence the concentrations of some of the gases.³¹ He, for example,~~
172 ~~is known to be~~ Particularly, He being enriched in the pore water of sediments by in-situ

173 production or groundwater input might be subject to variations in the mixing of the water
174 masses. Further, can O₂ be significantly consumed by the sediments. However, Ar and Kr
175 are not affected by sediment/water exchange.³²

176 The gas measurements were carried out near the center of the lagoon. Water was pumped
177 55 *m* from the sampling point at a water depth of 1 *m* to the onshore GE-MIMS system
178 by a submersible pump through a hard plastic tube (polyamide tubing; 66 *m* in length).
179 Mechanical filters and regular cleaning of the membrane contactors kept the flow rates high
180 to guarantee reliable gas measurements. The travel time of the water through the hoses was
181 estimated to be approximately 5 *min* which is negligibly small in comparison to the diurnal
182 variation.

183 Results and Discussion

184 Resolution and Sensitivity

185 The DGD method allows determination of gas exchange rates only within a certain range of
186 k/h values. Here we discuss the upper and lower limits of the determination of the transfer
187 velocity using the DGD approach, and elaborate on the constraining parameters.

188 We have run the model several times in a theoretical setting to determine the sensitivity
189 and resolution of the method. For that purpose a synthetic sinusoidal variation in the
190 water temperature simulate the diurnal heating and cooling. This pre-set temperature cycle
191 has a mean temperature value of 15 °C, a peak-to-peak amplitude of 2 °C, 6 °C, 10 °C,
192 16 °C or 20 °C and a 24 *h* period. $C_{eq,i}$ were calculated for a constant atmospheric pressure
193 of 1013.15 *hPa*. The expected water concentrations $C_{w,i}$ are modeled for a k/h -range of
194 ~~0—10 h^{-1} . $C_{w,i}$ and $C_{eq,i}$ are then compared to each other and evaluated in the light of the~~
195 ~~experimental precision of the gas measurements. 0—10 d^{-1} .~~

196 This synthetic data exercise ~~allows~~ allow us to derive upper and lower bounds for the
197 determination of the gas transfer velocities by comparing the parameters to the experimental

198 precision of the gas measurements. We define two quantities necessary to be resolved
 199 by the measurement setup. (D_i) is the maximum difference between the expected water
 200 concentration and the equilibrium concentration normalized to the mean equilibrium concentration
 201 of one period, $D_i = \frac{\max(|C_{w,i}(t) - C_{eq,i}(t)|)}{C_{eq,i}}$. We define (A_i) as the amplitude of the expected
 202 concentration normalized to the mean equilibrium concentration of the time series $A_i = \frac{\max(C_{w,i}(t)) - \min(C_{w,i}(t))}{C_{eq,i}}$

203 For very low k/h , $C_{w,i}$ approaches a constant value. The water concentrations will be
 204 approximately equal to the equilibrium concentration at the daily mean water temperature.
 205 ~~In this case, the experimental setup is not sensitive to changes in k/h .~~ The lower limit of
 206 resolution of k/h is shown in Fig. 1 for Ar and for the five different values of diurnal water
 207 temperature variation. ~~We define this lower limit as the point at which the relative diurnal~~
 208 ~~variation due to temperature ($\max(C_w) - \min(C_w)$).~~ ~~In this case, the experimental setup is~~
 209 ~~not sensitive to changes in k/h as the amplitude, A_{Ar} (yellow, right y-axis in Fig. 1), due~~
 210 ~~to temperature~~ becomes less than the analytical precision ~~of the gas measurements~~ (red line
 211 in Fig. 1; for Ar) ~~. This of the gas measurements.~~ The limit is higher for lower diurnal
 212 temperature differences as the concentration gradients are smaller. For a water temperature
 213 amplitude of $10^\circ C$ the lower limit is approximately $0.07 d^{-1}$ for Ar, $0.05 d^{-1}$ for N_2 and
 214 $0.1 d^{-1}$ for Kr. The smaller the temperature amplitude of the daily forcing the higher the
 215 minimum of k/h that can be reliably determined.

216 For high k/h , the gas concentrations in surface water rapidly approaches $C_{eq,i}$, such that
 217 the difference between $C_{w,i}$ and $C_{eq,i}$ gets small. Any further increase in k/h will not pro-
 218 duce detectable changes between the expected and the equilibrium concentration, leaving the
 219 method insensitive for large k/h . Fig. 1 shows the relative difference between equilibrium and
 220 in-situ concentrations for Ar as function of diurnal water temperature variation ($\Delta C_{eq/InSitu}$,
 221 D_{Ar} (blue, left y-axis). The upper limit of the method is the point at which the difference
 222 between the gas concentration in water expected concentration and the equilibrium concen-
 223 tration becomes smaller than the analytical precision. The upper limit of the method is,
 224 therefore, reached if D_{Ar} is smaller than the analytical precision. For a diurnal temperature

225 change of 10°C , the upper limit of k/h that can be reliably measured is approximately $4 d^{-1}$
226 for Ar, $9 d^{-1}$ for N_2 and $2 d^{-1}$ for Kr. The smaller the temperature amplitude the lower the
227 maximum of k/h that can be reliably determined.

228 The range of k/h values that can be reliably determined by Ar is therefore approxi-
229 mately $0.07 - 4 d^{-1}$ for a diurnal temperature variation of 10°C . ~~For an assumed water~~
230 ~~depth~~ Results for water depths of $0.2 m$ ~~the range of gas transfer velocity that can be~~
231 ~~reliably determined is approximately $0.015 - 1.6 m/d$ and $0.6 m$ are of $0.01 - 0.8 m/d$ and~~
232 $0.04 - 2.4 m/d$, respectively.

233 The ability to resolve differences in gas transfer velocity therefore depends on the mag-
234 nitude of diurnal water temperature variation, on the water depth, on the temperature
235 dependence of the solubility in water and on the measurement precision. The latter two
236 factors are specific to each gas species.

237 In summary, the range of gas transfer velocities that can be determined by the DGD
238 method falls well in the range of gas transfer velocities that are typically encountered in
239 natural waters (average for lakes and reservoirs $1.0 m/d$; global average $5.7 m/d$).³³

240 **Controlled Experiment**

241 The results of the equilibrium, the observed and the modeled gas concentrations for N_2 , Ar
242 and Kr in the controlled experiment are shown in Fig. 2. The large diurnal amplitude in
243 water temperature in the tub (up to 25°C) result in large variations in $C_{eq,i}$. The observed
244 $C_{w,i}$ are lagged and their amplitudes are damped relative to $C_{eq,i}$, as predicted by the model.
245 Concentration changes in the dissolved gas concentrations ~~relative to the mean~~ are as high as
246 45 % for Kr, 16 % for Ar and 13 % for N_2 relative to the lowest measured concentration. These
247 changes are the direct result of the different solubilities and the analytical uncertainties.

248 The model reproduces the measured concentrations for the gases very well. The best-fit
249 gas exchange rates are: $k_{Ar}^* = 0.29 \pm 0.01 m/d$, $k_{N_2}^* = 0.27 \pm 0.02 m/d$, $k_{Kr}^* = 0.39 \pm 0.06 m/d$.
250 Those values result in a ratio of $k_{N_2}^*/k_{Ar}^* = 0.93 \pm 0.02$, which is, within the uncertainty, the

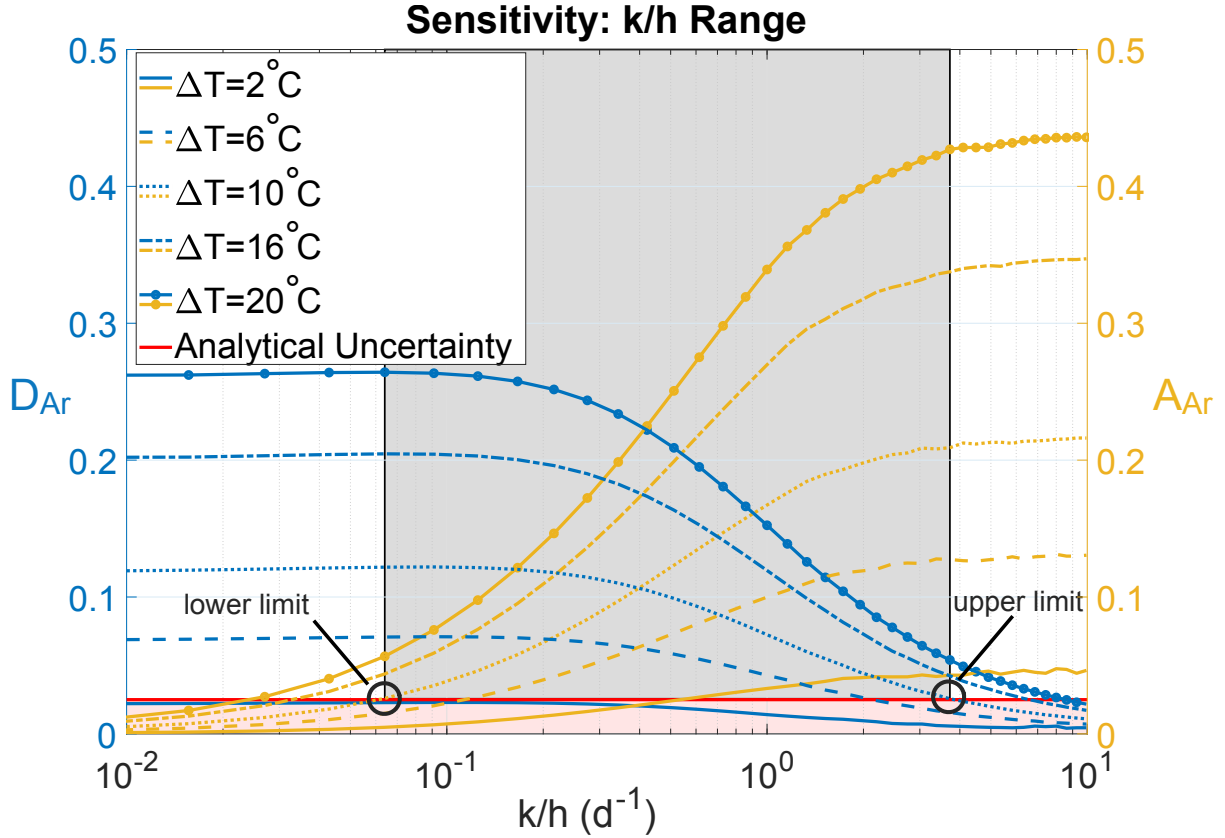


Figure 1: The maximal concentration difference between expected concentration in water and equilibrium concentration (D_{Ar}) (blue, left y-axis) and the ~~expected diurnal~~ amplitude of ~~the~~ water concentration (A_{Ar}) (yellow, right y-axis) both normalized to the mean equilibrium concentration ~~for Ar~~, shown for different water temperature amplitudes. High k/h results in a small difference between the expected and equilibrium concentrations, ~~hence, small~~ D_{Ar} . Where ~~this difference~~ D_{Ar} is less than the experimental precision (that for Ar is indicated by the red horizontal line), $C_{eq,i}$ and $C_{w,i}$ cannot be reliably differentiated, determining the upper limit on the k/h range. At low k/h the expected diurnal concentration amplitude, A_{Ar} , is less than the experimental precision. This, therefore, defines the lower limit for k/h determination. The range for $\Delta T = 10^\circ C$ (grey area and black circles) is approximately $0.07 - 4 d^{-1}$ for Ar with ~~a~~ ~~an~~ experimental uncertainty of 2.5%.

251 same as the expected value of 0.95 from Eq. 5 (Schmidt numbers for fresh water at $T = 20^\circ\text{C}$:
252 $S_{C_{Ar}} = 552$, $S_{C_{N_2}} = 612$, $S_{C_{Kr}} = 625^7$). For Kr the derived solution of the transfer velocity
253 matches with that scaled from Ar with the Schmidt number ratio ($k_{SC,Kr} = 0.27\text{ m/d}$) within
254 its 2σ confidence interval. $k_{SC,Kr}$ also fits the data well given the scattering of the data (Fig.
255 2). Due to the lower experimental precision the error of the estimated gas transfer velocity
256 is larger for Kr than for Ar and N_2 .

257 To illustrate the ability of the DGD method to reproduce $C_{w,i}$, model results for N_2 and
258 Ar are shown for $0.5 \cdot k_i^*$ and $1.5 \cdot k_i^*$. This exercise makes the case that the uncertainty of the
259 estimated transfer velocities for N_2 and Ar is significantly better than $\pm 50\%$, and mostly
260 falls in the range between $5 - 20\%$, depending also on the length of the measured time series.

261 The controlled experiment demonstrates the potential of the different gases to trace gas
262 exchange processes. Due to their low solubility and high atmospheric abundance, N_2 and Ar
263 are particularly powerful tracers for gas exchange. The analytical noise in Kr leads to a large
264 uncertainty in deriving the respective transfer velocity. Ar has a signal-to-noise ratio that is
265 only slightly higher than that of N_2 . These differences between gases are fully explained by
266 the abundance and the analytical performance of the applied GE-MIMS method to determine
267 gas concentrations.¹⁶

268 In summary, we interpret the controlled experiment as a proof of concept of the DGD
269 method, ~~especially for the lower gas transfer velocities commonly reported for inland waters~~
270 ~~and coastal zones.~~

271 **Field Study at La Palme Lagoon**

272 Fig. 3 shows the results of the equilibrium, the observed and the modeled gas concentrations
273 of the La Palme lagoon. The diurnal temperature variation was up to 10°C , significantly
274 less than in the tub experiment. For such smaller diurnal temperature amplitudes the exper-
275 imental errors of the Kr measurements are too large to estimate the gas transfer velocity in a
276 robust manner. Therefore, in the following only N_2 and Ar results are shown and discussed.

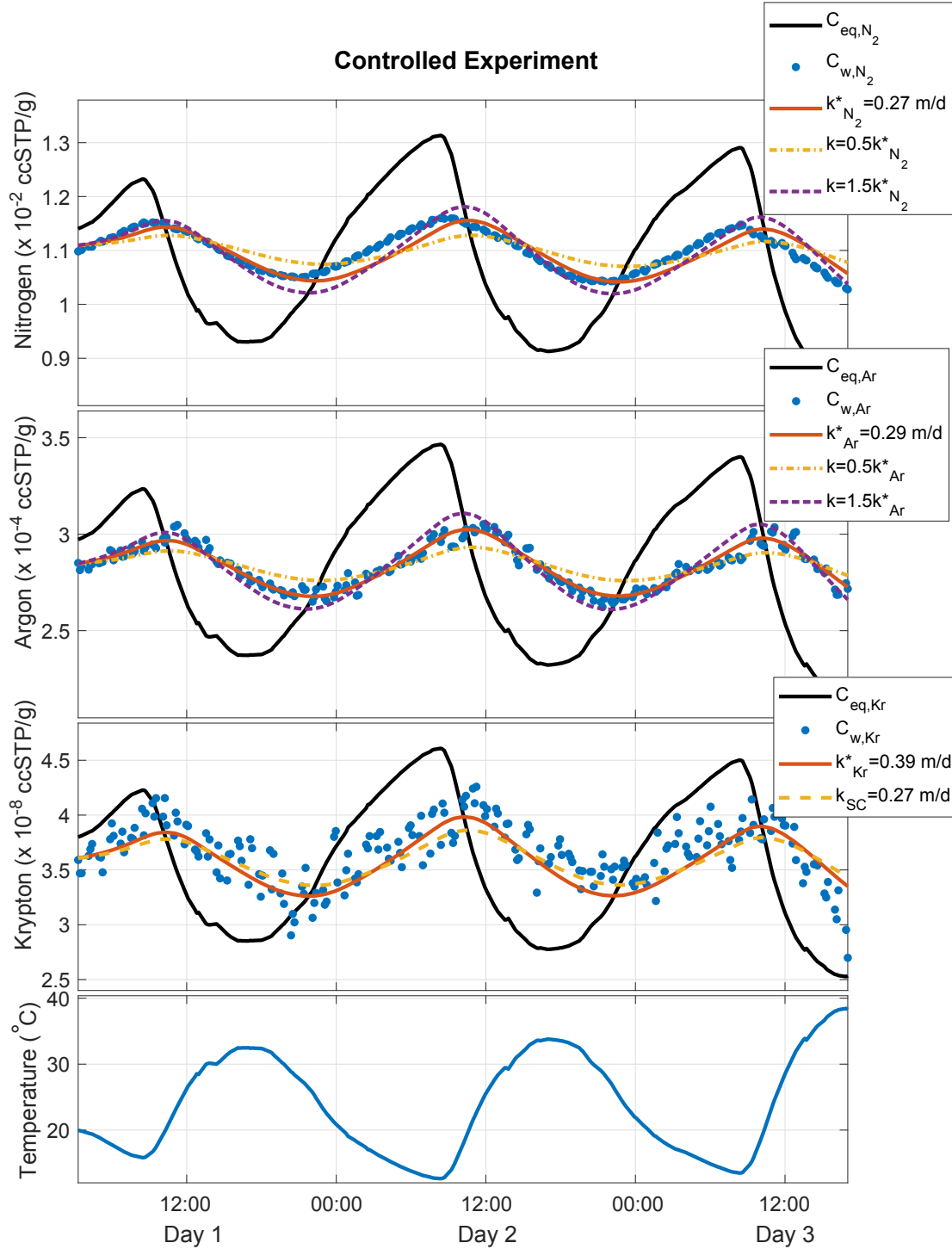


Figure 2: The equilibrium, the observed and the modeled concentrations for N_2 , Ar and Kr and the water temperature for the controlled experiment and the respective transfer velocities (k_i). The model fits the gas concentrations well. The derived gas exchange rates k^* are: $k_{N_2}^* = 0.27$ m/d, $k_{Ar}^* = 0.29$ m/d, $k_{Kr}^* = 0.39$ m/d. To illustrate the sensitivity of the DGD method, transfer velocities 50% larger and smaller than k_i^* are shown for N_2 and Ar. For Kr the result expected of the transfer velocity scaled from Ar with the Schmidt numbers is additionally shown (k_{SC} for Kr).

277 The model reproduces the observed data for N_2 remarkably well. Ar concentrations are
278 also reproduced correctly for a large period of the time series. However, in the morning
279 of the second day we observed a decrease in Ar concentrations which ~~we do not capture~~
280 are not captured by our simple model. The low concentration may relate to a specific
281 (but unidentified) event or process which affect the Ar but not the N_2 concentration. Such
282 deviation between the measured and the modeled concentration shows how valuable time
283 series of gas measurements over several days are, as they inform on additional processes that
284 affect atmospheric gases in aquatic systems besides atmospheric exchange. However, we have
285 no appropriate explanation for the observed deviation between the measured and predicted
286 Ar concentration.

287 For N_2 two periods with different response dynamics of the in-situ concentrations to the
288 diurnal heating can be observed (indicated with different colors in Fig. 3). For the first period
289 which lasts approximately for the first two and a half days the observed N_2 concentrations
290 are highly damped relative to the atmospheric equilibrium concentrations. For the second
291 period the dampening of the measured to the equilibrium concentrations is much smaller.
292 Further, the phase lag decreases from the first to the second period. Consequently, for the
293 two periods very differing transfer velocities prevail. For the first period: $k_{N_2}^* = 1.6 \pm 0.2 \text{ m/d}$.
294 For the second period: $k_{N_2}^* = 7.1 \pm 0.6 \text{ m/d}$. Leaving the described discrepancy on the second
295 day out for Ar, globally, the same behavior can be found in the Ar time series.

296 The measurement position within the lagoon is rather sheltered against wind (fetch of
297 approximately 50 m). Thus, during wind-calm conditions waves rapidly dissipate. During
298 the first period wind speeds were low (mean wind speed $\bar{u}_{10} = 2.9 \text{ m/s}$; u_{10} : measured wind
299 speed scaled to ten meters above the water surface³⁴), while during the second period wind
300 speeds more than three times higher were observed ($\bar{u}_{10} = 10.2 \text{ m/s}$). This change was also
301 found in the transfer velocity, and demonstrates the ability of the method to resolve different
302 weather conditions on time scales of hours to days.

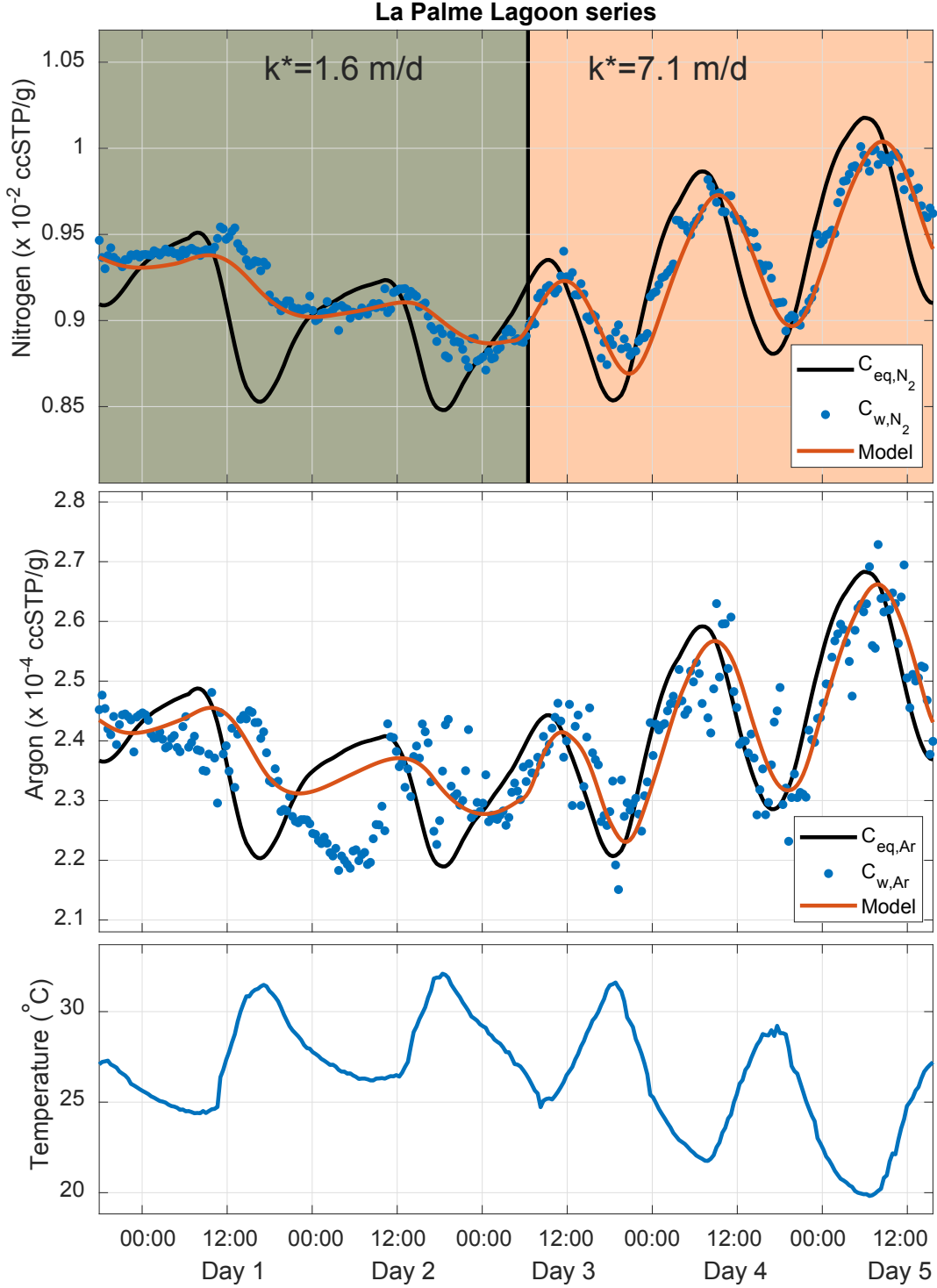


Figure 3: The equilibrium, the observed and the modeled concentrations for N_2 and Ar and the water temperature series of the water in La Palme Lagoon. The derivation of the transfer velocity for N_2 with the DGD method is split into two periods. The first 2.5 days (green) result in a transfer velocity of $k_{N_2}^* = 1.6 \pm 0.2 \text{ m/d}$, while the second 2.5 days (orange) result in $k_{N_2}^* = 7.1 \pm 0.6 \text{ m/d}$. Those phases are characterized by very different wind regimes with $\bar{u}_{10} = 2.9 \text{ m/s}$ for the first and $\bar{u}_{10} = 10.2 \text{ m/s}$ for the second phase.

303 Discussion

304 The controlled and the La Palme lagoon experiments demonstrate the capability of the
305 DGD method to quantify temporally changing gas exchange rates at specific locations and
306 on relative short time scales. The presented method allows the quantification of the transfer
307 velocity over the wide range of approximately ~~0.1–8 m/d~~0.05–9 m/d (for N₂), which covers
308 the typically observed range of gas transfer for surface waters. The quantifiable range in k/h
309 depends on the magnitude of the diurnal water temperature variation, the ~~water depth, the~~
310 temperature dependence of the gas solubility in water and on the measurement precision.

311 The selection of gases being used as tracers by our method depends on the environmental
312 processes the respective gases are undergoing and on the experimental setup. The noble gases
313 He, Ne, Ar, Kr, Xe and Rn are best suited due to their inert behavior, whereas the gases
314 O₂ and N₂ are subject to biochemical reactions. However, the noble gases He and Rn,
315 in contrast to Ar, Kr and Xe, are released from the sediments by radioactive decay and
316 their concentrations, therefore, depend on e.g. groundwater inflow and circulation of water
317 between surface water and sediments.

318 From a technical perspective of the noble gases, currently only He, Ar and Kr can be
319 analyzed quasi-continuously, whereas in-situ ~~measurements of~~measurement capability for Ne
320 and Xe using our GE-MIMS instrument remains to be developed. On-going improvements
321 of the experimental performance of (GE)-MIMS systems might increase the number of gases
322 that can be used to analyze air/water partitioning and, thus, greatly expand the determinable
323 range (and the accuracy) of k/h values.

324 Our experiments show that N₂ and Ar are most sensitive to gas transfer velocities under
325 field conditions given the available technology. N₂ yields the widest k/h range as it has the
326 best signal-to-noise ratio. However, N₂ is potentially non-conservative due to biogeochemical
327 processes, such as denitrification.

328 The DGD method works best for large daily temperature changes in the water; ~~a minimum~~
329 preferably a water temperature variation of 10 °C ~~should prevail~~prevails to get reliable re-

330 sults ~~for the~~ and to cover a relevant range of gas transfer velocities. ~~The method is therefore~~
331 ~~most suitable for water depths of~~ Such high variations are more likely to be found in shallow
332 waters with depths less than a few meters. ~~Deeper water is less likely to show strong diurnal~~
333 ~~temperature variations, and is also,~~ furthermore, deeper water is unlikely to be vertically
334 well mixed as assumed in our model. Additionally, local conditions can influence the diurnal
335 temperature cycles, including solar radiation, water residence time and heat absorption.
336 These impact the applicability of this method. In rivers, for example, where the method is
337 applicable in principle¹⁵, this temperature requirement is currently the limiting factor and
338 could be rare to find. Again, improvements in gas measurements expand the locations that
339 can be covered.

340 The DGD method can be used to quantify temporal variations in transfer velocities,
341 which can then be linked to environmental drivers of air-water exchange, such as wind or
342 river-flow-driven turbulence. For instance, measuring k_i over a few days with varying wind
343 speeds could be used to derive relationships between transfer velocity and wind speed in
344 shallow environments. It may also be possible to determine the influence of parameters
345 (e.g. precipitation) on near surface turbulence that are less frequently incorporated into the
346 estimation of the gas transfer velocity.

347 The mass spectrometer used in this study can cycle through multiple inlets on a time
348 scales of minutes, which allows automated analysis at several locations simultaneously. This
349 allows coverage of different geographic conditions at sites, that may be more complex than
350 the open ocean. Hence, site-specific parametrizations can be derived on several orders of
351 areal extents.

352 As the DGD method does not rely on the application of any artificial tracer, there is
353 no contamination of the environment. With additionally determined quantities e.g. tidal
354 influences, groundwater intrusion or deep water mixing a more complete description of a
355 study site is possible.

356 Alternative approaches for measuring air-water gas exchange are more labor intensive and

357 have limited temporal resolution. The DGD method presented here, thus has the potential
358 to greatly improve on the ability to measure air-water exchange in shallow waters.

359 **Acknowledgements**

360 We gratefully thank Aladin Andrisoa, Anne Brennwald, Marine David, Alexandra Lightfoot
361 and Valenti Rodellas for conducting the field measurements with us. [Furthermore, we thank](#)
362 [three anonymous reviewers for their constructive comments.](#)

363 This research is a contribution to the ANR @RAction chair medLOC (ANR-14-ACHN-
364 0007-01, T. Stieglitz) and Labex OT-Med (ANR-11-LABEX-0061, part of the “Investisse-
365 ments d’Avenir” program through the A/MIDEX project ANR-11-IDEX-0001-02), funded
366 by the French National Research Agency (ANR). PC acknowledges support from IMÉRA
367 (Institute of Advanced Studies), Aix-Marseille Université (Labex RFIEA and ANR “In-
368 vestissements d’avenir”).

References

- (1) Stieglitz, T. C.; van Beek, P.; Souhaut, M.; Cook, P. G. Karstic groundwater discharge and seawater recirculation through sediments in shallow coastal Mediterranean lagoons, determined from water, salt and radon budgets. *Marine Chemistry* **2013**, *156*, 73–84.
- (2) Cook, P. G.; Lamontagne, S.; Berhane, D.; Clark, J. F. Quantifying groundwater discharge to Cockburn River, southeastern Australia, using dissolved gas tracers ^{222}Rn and SF_6 . *Water Resources Research* **2006**, *42*, [W10411](#).
- (3) [Gleeson, T.; Manning, A. H.; Popp, A.; Zane, M.; Clark, J. F. The suitability of using dissolved gases to determine groundwater discharge to high gradient streams. *Journal of Hydrology* **2018**, *557*, 561–572.](#)
- (4) Cole, J. J.; Prairie, Y. T.; Caraco, N. F.; McDowell, W. H.; Tranvik, L. J.; Striegl, R. G.; Duarte, C. M.; Kortelainen, P.; Downing, J. A.; Middelburg, J. J.; Melack, J. Plumbing the Global Carbon Cycle: Integrating Inland Waters into the Terrestrial Carbon Budget. *Ecosystems* **2007**, *10*, 172–185.
- (5) Heinze, C.; Meyer, S.; Goris, N.; Anderson, L.; Steinfeldt, R.; Chang, N.; Quéré, C. L.; Bakker, D. C. E. The ocean carbon sink – impacts, vulnerabilities and challenges. *Earth System Dynamics* **2015**, *6*, 327–358.
- (6) Qiu, X.; Zhu, T.; Wang, F.; Hu, J. Air–Water Gas Exchange of Organochlorine Pesticides in Taihu Lake, China. *Environmental Science & Technology* **2008**, *42*, 1928–1932.
- (7) Wanninkhof, R. Relationship between wind speed and gas exchange over the ocean revisited. *Limnology and Oceanography: Methods* **2014**, *12*, 351–362.
- (8) Khadka, M. B.; Martin, J. B.; Kurz, M. J. Synoptic estimates of diffuse groundwater seepage to a spring-fed karst river at high spatial resolution using an automated radon measurement technique. *Journal of Hydrology* **2017**, *544*, 86–96.

- 393 (9) Ashton, I. G.; Shutler, J. D.; Land, P. E.; Woolf, D. K.; Quartly, G. D. A Sensitivity
394 Analysis of the Impact of Rain on Regional and Global Sea-Air Fluxes of CO₂. *PLOS*
395 *ONE* **2016**, *11*, e0161105.
- 396 (10) Ho, D. T.; Bliven, L. F.; Wanninkhof, R.; Schlosser, P. The effect of rain on air-water
397 gas exchange. *Tellus B* **1997**, *49*, 149–158.
- 398 (11) Ho, D. T.; Coffineau, N.; Hickman, B.; Chow, N.; Koffman, T.; Schlosser, P. Influence
399 of current velocity and wind speed on air-water gas exchange in a mangrove estuary.
400 *Geophysical Research Letters* **2016**, *43*, 3813–3821.
- 401 (12) Watson, A. J.; Upstill-Goddard, R. C.; Liss, P. S. Air–sea gas exchange in rough and
402 stormy seas measured by a dual-tracer technique. *Nature* **1991**, *349*, 145–147.
- 403 (13) Hall Jr., R. O.; Madinger, H. L. Use of argon to measure gas exchange in turbulent
404 mountain streams. *Biogeosciences* **2018**, *15*, 3085–3092.
- 405 (14) [Knapp, J. L.; Osenbrück, K.; Brennwald, M. S.; Cirpka, O. A. In-situ mass spectrometry
406 improves the estimation of stream reaeration from gas-tracer tests. *Science of The Total
407 Environment* **2019**, *655*, 1062–1070.](#)
- 408 (15) Sanford, W. E.; Casile, G.; Haase, K. B. Dating base flow in streams using dissolved
409 gases and diurnal temperature changes. *Water Resources Research* **2015**, *51*, 9790–
410 9803.
- 411 (16) Brennwald, M. S.; Schmidt, M.; Oser, J.; Kipfer, R. A Portable and Autonomous Mass
412 Spectrometric System for On-Site Environmental Gas Analysis. *Environmental Science*
413 *& Technology* **2016**, *50*, 13455–13463.
- 414 (17) Manning, C. C.; Stanley, R. H. R.; Lott, D. E. Continuous Measurements of Dissolved
415 Ne, Ar, Kr, and Xe Ratios with a Field-Deployable Gas Equilibration Mass Spectrom-
416 eter. *Analytical Chemistry* **2016**, *88*, 3040–3048.

- 417 (18) Chatton, E.; Labasque, T.; de La Bernardie, J.; Guihéneuf, N.; Bour, O.; Aquilina, L.
418 Field Continuous Measurement of Dissolved Gases with a CF-MIMS: Applications to
419 the Physics and Biogeochemistry of Groundwater Flow. *Environmental Science & Tech-*
420 *nology* **2016**, *51*, 846–854.
- 421 (19) Schwarzenbach, R. P.; Gschwend, P. M.; Imboden, D. M. *Environmental Organic Chem-*
422 *istry*; John Wiley & Sons, Inc., 2016.
- 423 (20) Kipfer, R.; Aeschbach-Hertig, W.; Peeters, F.; Stute, M. Noble Gases in Lakes and
424 Ground Waters. *Reviews in Mineralogy and Geochemistry* **2002**, *47*, 615–700.
- 425 (21) Weiss, R. The solubility of nitrogen, oxygen and argon in water and seawater. *Deep Sea*
426 *Research and Oceanographic Abstracts* **1970**, *17*, 721–735.
- 427 (22) Weiss, R. F.; Kyser, T. K. Solubility of krypton in water and sea water. *Journal of*
428 *Chemical & Engineering Data* **1978**, *23*, 69–72.
- 429 (23) Sander, R. Compilation of Henry’s law constants for inorganic and organic species of
430 potential importance in environmental chemistry. 1999.
- 431 (24) Jähne, B.; Münnich, K. O.; Bössinger, R.; Dutzi, A.; Huber, W.; Libner, P. On the
432 parameters influencing air-water gas exchange. *Journal of Geophysical Research* **1987**,
433 *92*, 1937.
- 434 (25) Etcheto, J.; Merlivat, L. Satellite determination of the carbon dioxide exchange coeffi-
435 cient at the ocean-atmosphere interface: A first step. *Journal of Geophysical Research*
436 **1988**, *93*, 15669–15678.
- 437 (26) Press, W. H.; Teukolsky, S. A.; Vetterling, W. T.; Flannery, B. P. *Numerical recipes*
438 *3rd edition: The art of scientific computing*; Cambridge university press, 2007.
- 439 (27) Savitzky, A.; Golay, M. J. Smoothing and differentiation of data by simplified least
440 squares procedures. *Analytical chemistry* **1964**, *36*, 1627–1639.

- 441 (28) Mächler, L.; Brennwald, M. S.; Kipfer, R. Membrane Inlet Mass Spectrometer for the
442 Quasi-Continuous On-Site Analysis of Dissolved Gases in Groundwater. *Environmental*
443 *Science & Technology* **2012**, *46*, 8288–8296.
- 444 (29) Mächler, L.; Brennwald, M. S.; Tyroller, L.; Livingstone, D. M.; Kipfer, R. Conquer-
445 ing the Outdoors with On-site Mass Spectrometry. *CHIMIA International Journal for*
446 *Chemistry* **2014**, *68*, 155–159.
- 447 (30) Rodellas, V.; Stieglitz, T. C.; Andrisoa, A.; Cook, P. G.; Raimbault, P.; Tam-
448 borski, J. J.; van Beek, P.; Radakovitch, O. Groundwater-driven nutrient inputs to
449 coastal lagoons: The relevance of lagoon water recirculation as a conveyor of dissolved
450 nutrients. *Science of The Total Environment* **2018**, *642*, 764–780.
- 451 (31) Cook, P. G.; Rodellas, V.; Stieglitz, T. C. Quantifying Surface Water, Porewater,
452 and Groundwater Interactions Using Tracers: Tracer Fluxes, Water Fluxes, and End-
453 member Concentrations. *Water Resources Research* **2018**, *54*, 2452–2465.
- 454 (32) Brennwald, M. S.; Vogel, N.; Scheidegger, Y.; Tomonaga, Y.; Livingstone, D. M.;
455 Kipfer, R. *The Noble Gases as Geochemical Tracers*; Springer Berlin Heidelberg, 2013;
456 pp 123–153.
- 457 (33) Raymond, P. A.; Hartmann, J.; Lauerwald, R.; Sobek, S.; McDonald, C.; Hoover, M.;
458 Butman, D.; Striegl, R.; Mayorga, E.; Humborg, C.; Kortelainen, P.; Dürr, H.; Mey-
459 beck, M.; Ciais, P.; Guth, P. Global carbon dioxide emissions from inland waters. *Nature*
460 **2013**, *503*, 355–359.
- 461 (34) Foken, T. *Micrometeorology*; Springer Berlin Heidelberg, 2017.